PAPER

The adsorption of a mixture of particles with non-additive interactions: a Monte Carlo study

O. A. Pinto,*[a] P. M. Pasinetti,[b] A. J. Ramirez-Pastor[b] and F. D. Nieto[b]

The adsorption of binary mixtures with non-additive lateral interactions has been studied through grand canonical Monte Carlo simulations in the framework of the lattice-gas model. The traditional assumption of additive lateral interactions is replaced with a more general one including non-pairwise interactions. It is assumed that the energy linking a certain atom with any of its nearest neighbors strongly depends on the state of occupancy in the first coordination sphere of such an adatom. The process has been monitored through the adsorption isotherms and the differential heats of adsorption. Different combinations of both inter- and intra-species interactions have been considered in the analysis. Interesting behaviors were observed and discussed in terms of the low temperature phases formed in the system.

I. Introduction

The adsorption process of a mixture of gases on solid surfaces is a topic of great interest mainly from the technological point of view, due to its importance in new developments in fields like gas separation and purification.[1–4] This problem has been theoretically[5–12] and experimentally[11–15] studied for many years, however some aspects of the problem remain unexplored.

As in any adsorption process, a complete analysis of the behavior of gas molecules under the influence of an adsorbent requires taking into account the effect of the lateral interactions between each species of the mixture.[1,16–18] An exact treatment of this problem, including adsorbate–adsorbate interactions, is unfortunately not yet available and, therefore, the theoretical description of mixture adsorption relies on simplified models.[4] Valuable contributions have been made in this direction by the group of Y. K. Tovbin and co-workers, who studied pure and mixed adsorption in the presence of lateral interactions and surface heterogeneity.[19–22] On the basis of a new theoretical method (the so-called fragment cluster method) and by using different approximations in the context of the lattice-gas theory, the authors investigated the main adsorption functions (isotherms and heats of adsorption) and the effects of the phase transitions occurring in the system.

In the case of mixtures, the experimental approach is a much more demanding problem. While for pure components the number of adsorbed molecules can be determined accurately by simply weighing the sample, for mixtures one has to carry out additional experiments to determine the composition of the sample. This is one of the reasons for the lack of mixture adsorption data.

In this framework, the Monte Carlo (MC) simulation method[23–27] is a way of overcoming these experimental and theoretical complications. The MC technique is a valuable tool for studying surface molecular processes, which has been extensively used to simulate many surface phenomena including adsorption,[28] diffusion,[29] reactions, phase transitions,[30] etc. Here we will try to demonstrate that numerical simulations, combined with a correct theoretical interpretation of the results, can be very useful to obtain a very reasonable description of the adsorption of interacting binary mixtures on 2D square lattices.

One way of introducing more complex adsorbate–adsorbate interactions is by considering non-pairwise interactions in terms of non-additivity. In fact, the deviation in the additive behavior appears to be especially significant in the case of chemisorption where the valence electrons are either concentrated to form a single bond between two isolated atoms or shared among all neighbors which are occasionally occupying sites in the first coordination shell of the central atom.[31–35]

Among the effects caused by non-additive interactions, it is possible to mention:[34,35] (i) the particle-vacancy symmetry (valid for additive interactions) is broken and, consequently, the adsorption thermodynamic quantities (adsorption isotherms, configurational entropy, differential heat of adsorption, etc.) are asymmetric with respect to half coverage; (ii) a rich variety of ordered structures are observed in the adlayer; (iii) an ordered structure consisting of groups of particles adsorbed along k adjacent sites (called k-mers) is observed at high coverage; and (iv) for repulsive coupling, first- and

[a] *Centro de Investigaciones y Transferencia de Santiago del Estero, (CITSE-CONICET) Universidad de Santiago de Estero, RN 9 Km 1125 Villa el Zanjón, Santiago del Estero, CP 4206 Argentina. E-mail: oapinto@unsl.edu.ar; Fax: +54-385-4509504; Tel: +54-385-4509504*

[b] *Departamento de Física, Instituto de Física Aplicada, Universidad Nacional de San Luis, CONICET, Ejército de Los Andes 950, D5700HHW San Luis, Argentina*

second-order phase transitions occur in the adsorbate at different concentrations.

Non-additive adsorbate–adsorbate interactions have been recognized in several experimental systems, such as H on Pd(100), O on W(110), and H on Fe(110), just to name a few of them.[36–42] Another evidence of non-additivity is the tendency to dimer formation as observed, for example, in the adsorption of Cu and Ni on W(110) for particular coverage values according to thermal desorption spectroscopy analysis.[43] The adsorption of H on graphene (by STM studies) is another example of dimer formation associated with surface restructuring.[44]

The consequences of considering non-pairwise (non-additive) interactions in the adsorption thermodynamics have been studied for long time. In fact, statistical mechanics of adsorbed monolayers has been a subject of analytical treatment by means of mean field[32,33] and quasichemical[31] approximations. In most of the cited papers, the study has been restricted to some special cases mainly including attractive interactions. However, the case of repulsive interactions is also of interest mainly because (a) experimental phase diagrams corresponding to many systems in the presence of surface restructuring are explained in terms of those interactions;[45–47] (b) the tendency to dimer formation, which seems to be relevant in several systems mentioned above, can be predicted on the basis of such kind of coupling; and (c) a rich variety of non-symmetrical phase diagrams (around half coverage) can be described. Some efforts in this direction include the study of adsorption of monomers[34–35,48] and linear k-mers[49] with repulsive non-additive lateral interactions on substrates of different connectivity.

In the specific case of adsorption of a single monomeric species on square lattices, the most relevant results can be summarized as follows: (i) the occurrence of experimentally observed structures[43] formed by clusters of two or four particles (called dimeric and tetrameric phases) can be corroborated by simulation in a certain range of coverage and interaction parameters; and (ii) a change in the stability (weakening or reinforcement) of the $c(2 \times 2)$ structure is observed depending on the parameter of non-additivity. This is evidenced by the behavior of the different thermodynamic functions, for example, by a narrowing (or widening) of the half coverage plateau in the adsorption isotherms. Similar results have been found in adsorption studies on nanotube bundles.[48]

In this context, the main aim of this manuscript is to extend earlier work on adsorption with non-additive interactions to include more than one adsorbed species. The present paper is a natural extension of previous studies in which non-additive interactions have been included in the context of the lattice theory.[31–35,48,49] The observed occupation by adsorbed particles of preferred sites of a lattice, commensurate with the substrate surface, is a justification for the use of the lattice theory.[33]

It is clear that a complete analysis of this field is a quiet difficult subject. For this reason, the understanding of simple models with increasing complexity might be a help and a guide to establish a general framework for the study of this kind of systems. In this line, our objectives are (i) to identify and characterize the most prominent features of the effect of non-additive interactions on the thermodynamic quantities describing the adsorption of binary mixtures; (ii) to draw general conclusions on the effect of non-additive interactions on adsorption and competition; and (iii) to provide the basis for the evaluation of experimental findings in the presence of mixtures with non-additive lateral interactions.

The paper is organized as follows. In Section II, the lattice-gas model including non-additive interactions between adatoms is described. Section III presents the basis of the MC simulations. Section IV shows the results for the adsorption thermodynamics from MC simulations. Finally, in Section V the conclusions and future perspectives are given.

II. The non-additive model

In the context of the lattice-gas model, the adsorption of two different species, A and B, on a homogeneous surface with a square geometry consisting of M ($=L \times L$) sites has been studied. Periodic boundary conditions have been considered and multi-deposition is prohibited. There are two kinds of energies involved: adsorbate–adsorbent interaction, ε, and lateral nearest-neighbor (NN) interactions, which can be separated in inter-species, w_{AB}, and intra-species, w_{AA} and w_{BB}. The substrate is exposed to a mixed gas of A and B particles, whose state is characterized by the chemical potentials μ_A and μ_B and temperature T. The occupation variable c_i is equal to zero if site i is empty, and is equal to +1 (-1) if it is occupied with species A (B). Thus, the Hamiltonian of the system can be written as

$$
\begin{aligned}
H = &\sum_{i}^{M} \sum_{l \in (\mathrm{NN},i)} \left[w_{AA} \delta_{c_i,c_l,1} + w_{BB} \delta_{c_i,c_l,-1} \right. \\
&\left. + w_{AB} \left(\delta_{c_i,1} \delta_{c_l,-1} + \delta_{c_i,-1} \delta_{c_l,1} \right) \right] \\
&+ \varepsilon \sum_{i}^{M} \left(\delta_{c_i,1} + \delta_{c_i,-1} \right) - \sum_{i}^{M} \left(\mu_A \delta_{c_i,1} + \mu_B \delta_{c_l,-1} \right),
\end{aligned} \tag{1}
$$

where $l \in (\mathrm{NN},i)$ run on all NN sites of site i and δ is the Kronecker function.

As discussed in the previous section, the term non-additive refers here to a binding energy between two atoms depending on the surrounding where those two atoms are immersed. In this sense, there are twelve possible lateral energies, $w_{AA}^1 \ldots w_{AA}^z$, $w_{AB}^1 \ldots w_{AB}^z$ and $w_{BB}^1 \ldots w_{BB}^z$, which could be present (taking $z = 4$, the coordination number for the square lattice). As an example, Fig. 1(a) shows a possible configuration of particles A and B and their contribution to the configurational energy of the system.

In general, the dependence of the lateral interaction on the number of neighbours is usually not known and is expected to be different in specific cases. A commonly adopted rule to consider non-additivity consists of a coupling energy depending linearly on the number of NN particles. Although physically reasonable, it might not be the most general way to express the dependence of the coupling energies. Moreover, the number of unknown parameters, w_{xx}^m, is thus drastically reduced and the study can be carried out in a simple manner.
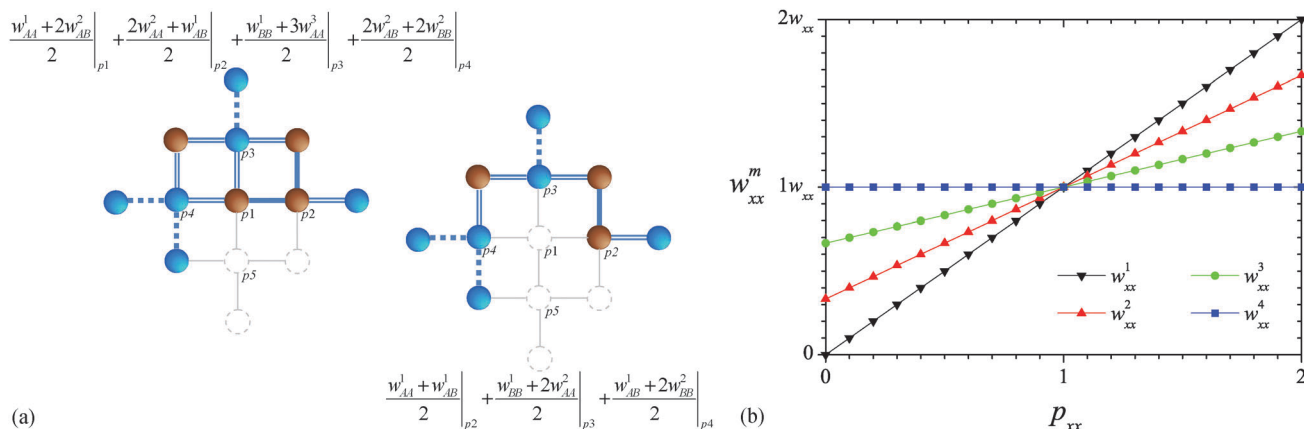
$$\left.\frac{w_{AA}^1 + 2w_{AB}^2}{2}\right|_{p1} + \left.\frac{2w_{AA}^2 + w_{AB}^1}{2}\right|_{p2} + \left.\frac{w_{BB}^1 + 3w_{AA}^3}{2}\right|_{p3} + \left.\frac{2w_{AB}^2 + 2w_{BB}^2}{2}\right|_{p4}$$

$$\left.\frac{w_{AA}^1 + w_{AB}^1}{2}\right|_{p2} + \left.\frac{w_{BB}^1 + 2w_{AA}^2}{2}\right|_{p3} + \left.\frac{w_{AB}^1 + 2w_{BB}^2}{2}\right|_{p4}$$

Fig. 1 (a) A possible local configuration of A particles (red), B particles (blue) and empty sites, with a red particle in the center (left) and the same configuration with the center empty (right). In the expressions, each term corresponds to the coupling energy of one of the particles, as indicated (the factor 1/2 is to prevent the double counting in the total energy). (b) Dependence of the coupling energies on the non-additive parameter.

To quantify this, a non-additive parameter is defined, $p_{xx} = \frac{w_{xx}^1}{w_{xx}^z},$[31–33] as a measure for the ratio of the strongest to the weakest possible coupling in the system (where xx stands for AA, BB or AB). For m NN particles, the linear non-additive expression is:

$$\frac{w_{xx}^m}{w_{xx}} = \frac{p_{xx}z - 1}{z - 1} - m\frac{p_{xx} - 1}{z - 1} \tag{2}$$

where w_{xx} becomes the energy parameter for the xx combination. For clarity, Fig. 1(b) shows, for $z = 4$, the dependence of the coupling on the non-additive parameter. When $p_{AA} = p_{AB} = p_{BB} = 1$ the system recovers the additive form, in accordance with previous results.[50] In the case $w_{AB} = w_{BB} = 0$, the model reproduces the adsorption results of just one species.[34]

III. Monte Carlo simulation method

The adsorption process is simulated through MC simulations in the grand canonical ensemble.[28] As mentioned above, the substrate is exposed, at temperature T, to an ideal gas phase consisting of a binary mixture of particles A and B, with chemical potentials μ_A and μ_B, lateral interaction energies w_{AA}, w_{AB} and w_{BB}, and non-additive parameters p_{AA}, p_{AB} and p_{BB}. The adsorption–desorption process starts when a site is chosen at random and an attempt is made to change its occupancy state with a probability given by the Metropolis rule.[51,52] A Monte Carlo step (MCs) is achieved when M sites (being $M = L \times L$, the total number of lattice sites) have been tested to change their occupancy state. The equilibrium state is reached after discarding 10^5 MCs, and averages are taken over the next 10^5 MCs. At low temperatures, up to 10^6 MCs had to be used in order to let the system relax from metastable states.

The partial and total adsorption isotherms are obtained as

$$\theta_A(\mu_A, \mu_B) = \frac{\langle N_A \rangle}{M}, \ \theta_B(\mu_A \mu_B) = \frac{\langle N_B \rangle}{M}, \tag{3}$$

and

$$\theta(\mu_A, \mu_B) = \frac{\langle N_A + N_B \rangle}{M} = \frac{\langle N \rangle}{M}, \tag{4}$$

where the brackets denote the time average over the MC simulation runs. N_A [N_B] and N denote the number of adsorbed A [B] molecules and the total number of adsorbed particles, respectively. Accordingly, θ_A [θ_B] and θ represent the partial surface coverage of the A [B] species and the total surface coverage, respectively. Other interesting quantity is the differential heat of adsorption q_x for the species x, defined as[53–55]

$$q_x = -\frac{\partial u}{\partial \langle N_x \rangle} \tag{5}$$

where u is the energy of the adsorbed phase. Using basic relationships from the thermodynamics of adsorption and expressing the derivatives as fluctuations in the grand canonical ensemble, the following forms for the differential heats of adsorption can be obtained:[27,28]

$$q_A = -\frac{\Phi_A S_B - \Phi_B[\langle N_A N_B \rangle - \langle N_A \rangle \langle N_B \rangle]}{S_A S_B - [\langle N_A N_B \rangle - \langle N_A \rangle \langle N_B \rangle]^2}, \tag{6}$$

$$q_B = -\frac{\Phi_B S_A - \Phi_A[\langle N_A N_B \rangle - \langle N_A \rangle \langle N_B \rangle]}{S_A S_B - [\langle N_A N_B \rangle - \langle N_A \rangle \langle N_B \rangle]^2}, \tag{7}$$

where $\Phi_{A[B]} = \langle U N_{A[B]} \rangle - \langle U \rangle \langle N_{A[B]} \rangle$ and $S_{A[B]} = \langle N_{A[B]}^2 \rangle - \langle N_{A[B]} \rangle^2$.

IV. Results

The study will be centered on the case of repulsive lateral interactions where a rich variety of phases occur in the system. The computational simulations have been developed for square $L \times L$ lattices with $L = 128$ and periodic boundary conditions. In addition, the interaction energy of the substrate will be neglected ($\varepsilon = 0$) without any loss of generality, given that the surface considered is homogeneous. The finite-size effects on the adsorption properties were investigated by considering systems of increasing sizes (ranging between $L = 60$ and $L = 256$).
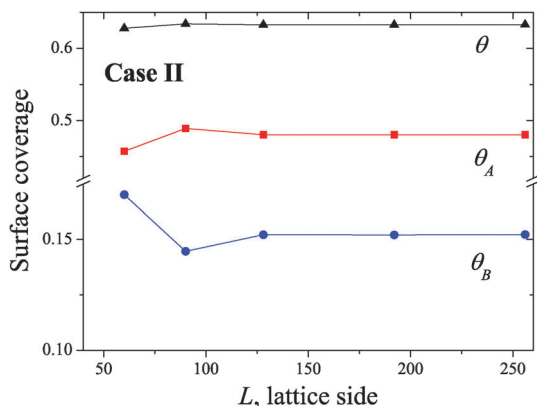
Fig. 2 Surface coverage (θ_A, θ_B and θ), as a function of the lattice side L, for $\mu_B = \mu_A = 44.0$, $w_{AA} = w_{AB} = w_{BB} = 15$, $p_{AB} = p_{BB} = 1$ and $p_{AA} = 0.2$ (Case II). As can be observed, finite-size effects are negligible for $L = 128$.

As an example of such studies, Fig. 2 shows, for a typical case ($\mu_B = \mu_A = 44.0$, $w_{AA} = w_{AB} = w_{BB} = 15$, $p_{AB} = p_{BB} = 1$ and $p_{AA} = 0.2$), how the partial and total coverage varies with the lattice size. As can be observed, finite-size effects are negligible from a system size of $L = 128$. In order to simplify the analysis of the whole phase space, which includes a wide range of values of w_{xx} and p_{xx}, the study is divided into three cases:

Case I: $\mu_B = 0$, $w_{AA} > 0$, $w_{AB} = w_{BB} = 0$, $p_{AB} = p_{BB} = 1$ and $p_{AA} \neq 1$.

Case II: $\mu_B = \mu_A$, $w_{AA} = w_{AB} = w_{BB} > 0$, $p_{AB} = p_{BB} = 1$ and $p_{AA} \neq 1$.

Case III: $\mu_B = \mu_A$, $w_{AA} = w_{BB} > 0$, $w_{AB} < 0$, $p_{AA} = p_{BB} = 1$ and $p_{AB} \neq 1$.

To start describing Case I, the chemical potential of one of the components is held fixed throughout the adsorption process, $\mu_B/k_BT = 0$, while μ_A/k_BT is changed, as is usually assumed in the studies of gas mixture adsorption.[20–22]

Fig. 3 shows the adsorption isotherms for both species, as indicated. The additive situation ($p_{AA} = 1$) is considered in the first place. As $\mu_A/k_BT \rightarrow -\infty$, A particles are no longer present ($\theta_A = 0$), whereas B particles are randomly deposited at $\theta_B = 1/2$ as can be expected from the Langmuir isotherm ($w_{BB}/k_BT = 0$) at $\mu_B/k_BT = 0$.[52] As the surface coverage of the A species increases, the B particles are expelled out of the surface. A broad plateau appears at $\theta_A = 1/2$ corresponding to the formation of a $c(2 \times 2)$ ordered structure as is expected for repulsive monomers. However, in this structure each A particle can have any of its NN sites either empty or occupied by a B particle. The coverage of the B species decreases to a plateau at $\theta_B = 1/4$, as the available space for this species has been reduced to half of the total. As the chemical potential μ_A/k_BT continues increasing, the A particles end up filling the lattice expelling completely the B particles.

Considering now the effects of non-additivity ($p_{AA} \neq 1$), the first part of the isotherms have the same general behavior, except for a narrowing of the plateaus at half coverage for values of $p_{AA} < 1$, which can be explained because the lateral interactions are weaker and the order is easily broken. At values of p_{AA} near 0.2, a new plateau is formed at $\theta_A = 2/3$, which corresponds to a zig–zag structure of A particles, also referred
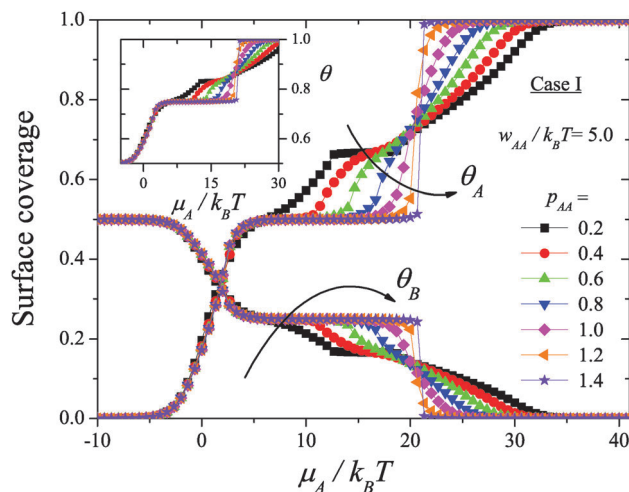

Fig. 3 Total (inset) and partial adsorption isotherms for Case I. The partial isotherms are labeled by A and B.

as a dimer-like or a *dimeric* structure from its similarity to structures observed in the adsorption of dimers. This structure becomes more stable as p_{AA} tends to zero, and is a purely non-additive effect. In the same direction, the isotherms of the B species present plateaus at $\theta_B = 1/4$ and $\theta_B = 1/6$, occupying in both cases the half of the vacant sites.

For $p_{AA} > 1$, a broadening of the plateaus, with respect to the additive case, is observed in the adsorption isotherms at the partial coverage $\theta_A = 1/2$ ($\theta_B = 1/4$). Then, the curves present a discontinuity from $\theta_A = 1/2$ to full coverage, as an evidence of a condensation process. This condensation can be explained because the system minimizes its free energy when A particles fill the surface. To conclude the analysis of Fig. 3, the inset shows the total adsorption isotherm. In the description made so far, B particles are confined to occupy half of the sites not occupied by the A particles.

Fig. 4 shows the extreme case of $p_{AA} = 0.2$ and $w_{AA}/k_BT = 20.0$. Total and partial adsorption isotherms are plotted in part (a).
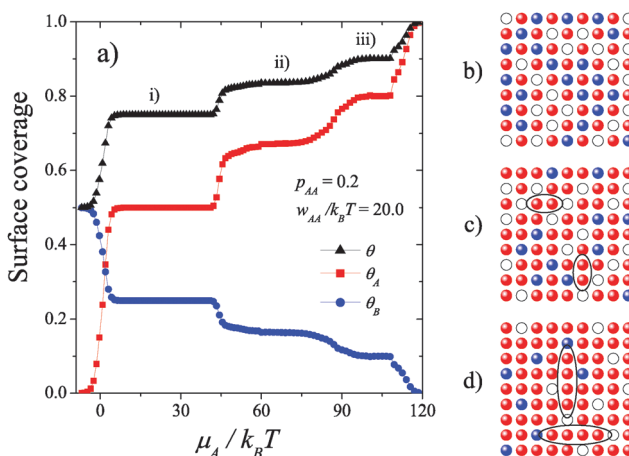

Fig. 4 (a) Total and partial isotherms for $p_{AA} = 0.2$. (b)–(d) are snapshots of the ordered structures corresponding to each plateaus of the total isotherm. Red circles represent A particles, blue circles correspond to B particles and white circles represent empty sites. The ellipses indicate the dimer and tetramer associations.

Besides the plateaus previously described, a new plateau appears at the coverage $\theta_A = 4/5$, which was previously reported in the case of the adsorption of a single monomeric species in ref. 34. In the same figure, the plateaus are leveled from (i) to (iii), showing on the right side a snapshot of the structures appearing in the adlayer in each case. For the first plateau, $\theta = 3/4$, red circles represent A particles, blue circles correspond to B particles and white circles represent the empty sites [see Fig. 4(b)]. As can be observed, A particles are ordered, forming a $c(2 \times 2)$ structure, whereas B particles fill half of the empty sites. Fig. 4(c) shows the structure corresponding to the second plateau, $\theta = 5/6$, consisting of the zig–zag ordering previously described: each A particle has two nearest neighbors of the same species (the ellipses mark a possible dimer association). The adsorption of B particles perturbs the complete formation of the A structure.

Finally, the snapshot of the last plateau ($\theta = 11/12$) is shown in Fig. 4(d), where A particles are bonded to three nearest neighbor particles of the same species. The resulting structure resembles that observed in the adsorption of tetramers (the so-called tetramers are indicated by ellipses). In all structures, B particles occupy the half of the available sites and, due to steric interactions, induce imperfections in the formation of the structures.

Another important quantity, which can also be measured in experiments, is the differential heat of adsorption, obtained here from eqn (5) and (6). Fig. 5(a) shows the differential heat of adsorption corresponding to the A species *versus* the total coverage, for the same conditions of Fig. 3. Since B particles have no interactions, q_B is zero in all the range of coverage.

In the case of the A particles, a more complex behavior is observed. Namely, for $p_{AA} < 1.0$, marked steps appear at coverage values in which the structures are formed. For the additive case ($p_{AA} = 1.0$), the step is formed at $q_A = -20.0$. These singularities show a dependence on p_{AA}. For $p_{AA} = 0.2$ the last step is not observed at this value of energy, but it is visible at stronger lateral energies like $w_{AA}/k_BT \geq 10.0$. For $p_{AA} > 1$ a discontinuity from $\theta = 3/4$ to $\theta = 1$ is observed, in correspondence with the condensation discussed in the isotherms.

In Fig. 5(b), the differential heat of adsorption for $p_{AA} = 0.6$ and several values of w_{AA}/k_BT are presented. The figure shows

that the step at 3/4 is more marked as the lateral energy is increased. In addition, an incipient step corresponding to the *tetrameric* structure is observed around $\theta = 0.8$ for $w_{AA}/k_BT = 10.0$ (black arrow marks this).

Considering now Case II, the chemical potentials of both components are driven together. Fig. 6(a) shows the partial adsorption isotherm of the A species for $w_{AA} = w_{AB} = w_{BB} = 5.0$ k_BT and several values of p_{AA}. For the additive case, A and B species are energetically indistinguishable, and the system behaves as a single component. In fact, a $c(2 \times 2)$ structure is formed with a mixture of both species with $\theta_A = \theta_B = 1/4$, and the total isotherm shows a plateau at half coverage (not shown here for simplicity). Values of p_{AA} less than unity lead to a narrow first plateau, indicating a weakening of that structure.

As the coverage of the A species increases, a zig–zag structure is formed in the adsorbate, causing the expulsion of the B particles. This process has a limit recognized by a minimum in the isotherm of the B species, as can be seen in the inset of Fig. 6(a). Both the expulsion of the B particles and the maximum coverage achieved by the A particles depend on how much the dimeric structure has been reinforced (*i.e.* on the value of p_{AA}). For increasing the values of the chemical potential, the reinsertion of B particles, rather than having only A particles adsorbed on the substrate, is more convenient. On the other hand, as p_{AA} tends to zero, the coverage of the zig–zag structure tends to 2/3 as would be expected in the adsorption of a single non-additive species.

In the analysis of the differential heat of adsorption [Fig. 6(b)], only the A species is considered, since both species have a similar behavior. In all cases, a marked step appears at half coverage. For $p_{AA} < 1.0$, a second step is observed, in concordance with the adsorption isotherms. The situation for $p_{AA} > 1$ is different. Once the structure $c(2 \times 2)$ is formed, the insertion of B particles is preferred due to the energies involved [$w_{AB} < w_{AA}^1(p_{AA})$]. Note that the AB interactions are additives.

To clarify the previous discussion, Fig. 7(a) shows the adsorption isotherms for $p_{AA} = 0.2$ and $w_{AA} = w_{BB} = w_{AB} = 15.0$ k_BT. In this figure it can be observed that both species are
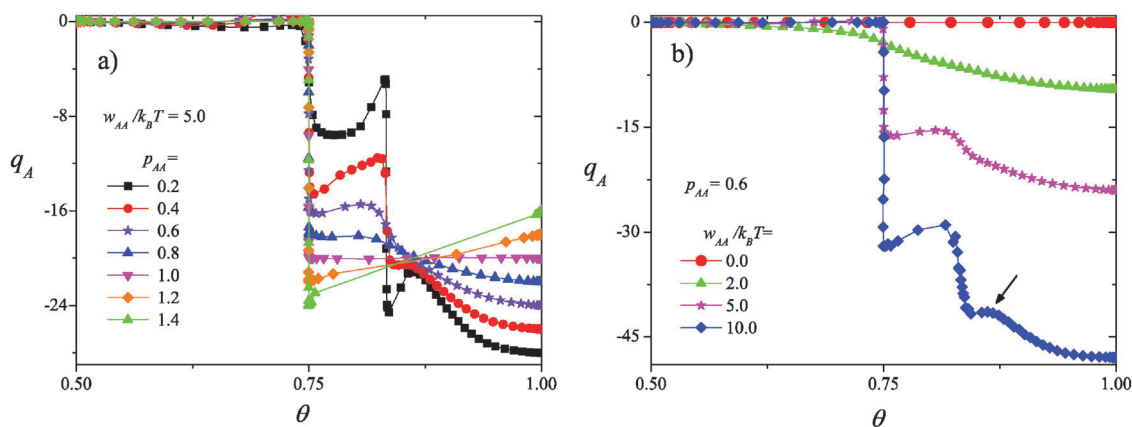

Fig. 5 Differential heat of adsorption for the A species. (a) As a function of p_{AA}. (b) For $p_{AA} = 0.6$ and different values of w_{AA}/k_BT.
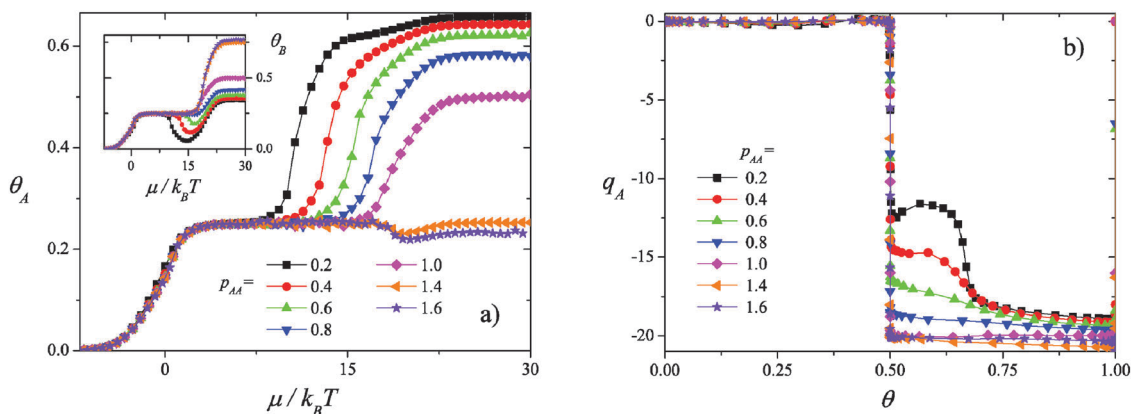
Fig. 6 (a) Partial adsorption isotherms for the A species and different values of the non-additive parameter for Case II. Inset: partial adsorption isotherms for the B species. (b) Differential heat of adsorption for the A species.
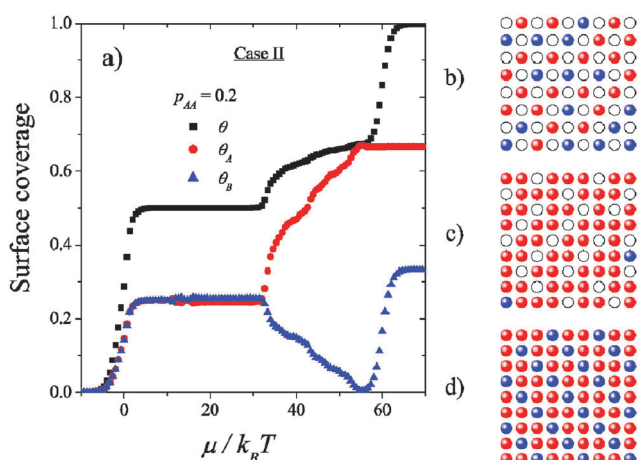

Fig. 7 (a) Total and partial adsorption isotherms for p_{AA} = 0.2. (b)–(d) are snapshots of the ordered structures corresponding to θ = 1/2, 2/3 and 1.0, respectively. Red circles represent A particles, blue circles correspond to B particles and white circles represent empty sites.
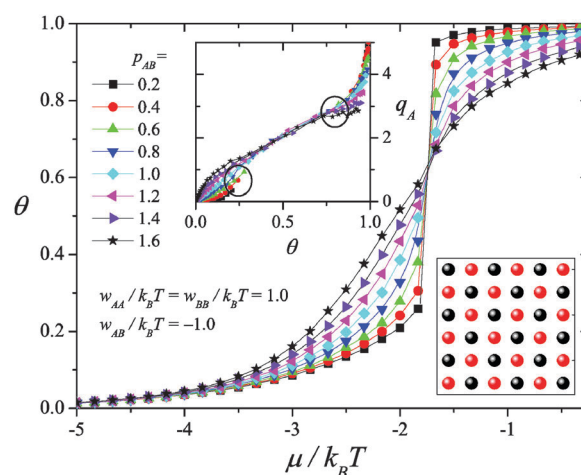
Fig. 8 Total adsorption isotherms at different values of p_{AB} for Case III. Inset: differential heat of adsorption for the A species (the ellipses indicate the presence of jumps in the curves).

deposited randomly forming a $c(2 \times 2)$ structure at θ = 1/2. The dimeric structure is formed at $\theta \approx 2/3$ and practically all the B particles are expelled at $\mu/k_BT \approx 55.0$. As μ/k_BT increases, the B particles complete the empty sites in the zig–zag structure. Fig. 7(b)–(d) show snapshots at θ = 1/2, 2/3 and 1.0, respectively.

Finally, the condition $w_{AA}/k_BT = w_{BB}/k_BT$ = 1.0 and a non-additive interspecies interaction are considered in Case III. The corresponding results for the total adsorption isotherm are presented in Fig. 8. From an energetic point of view, it is easy to understand the situation at full coverage, where a dimer association of A and B species (formation of an AB heterodimer) occurs in the adlayer. Accordingly, a $c(2 \times 2)$ ordered structure is formed by particles of one species surrounded by particles of the other species [see a snapshot in the inset].

For p_{AB} < 1.0, discontinuities associated with condensation are observed. The transition temperature from the inflexion point of the isotherm is a function of the non-additive parameter p_{AB}. For p_{AB} > 1.0, the curves look like a sigmoid. It is worth mentioning that, for w_{AB}/k_BT < −1.0 and p_{AB} > 1.0, a

jump associated with a condensation process is also observed (not shown here for simplicity). The differential heat of the A species is shown in the inset of Fig. 8 (B species presents the same behavior). The curves for p_{AB} < 1.0 have discontinuities in correspondence with the isotherms (as indicated by black circles), whereas for p_{AB} > 1.0 the curves are continuous. In this case, and even though two different classes of monomers are deposited, the mixture has a similar behavior to the adsorption of heterodimers with attractive interactions.

Finally, it is interesting to discuss the behavior of mixtures in a one-dimensional system. For this purpose, the substrate has been modeled as a chain of L sites (L = 1000) under periodic boundary conditions. This can be a good approximation for adsorption on low-dimensional systems, such as nanotube bundles.[56–58] For Case I, Fig. 9(a) shows the adsorption isotherms of both species, as is indicated. Interestingly, the isotherm behavior is rather the same as in the two dimensional system. The first plateau of the A species corresponds to a filling where each particle is separated from each other, corresponding
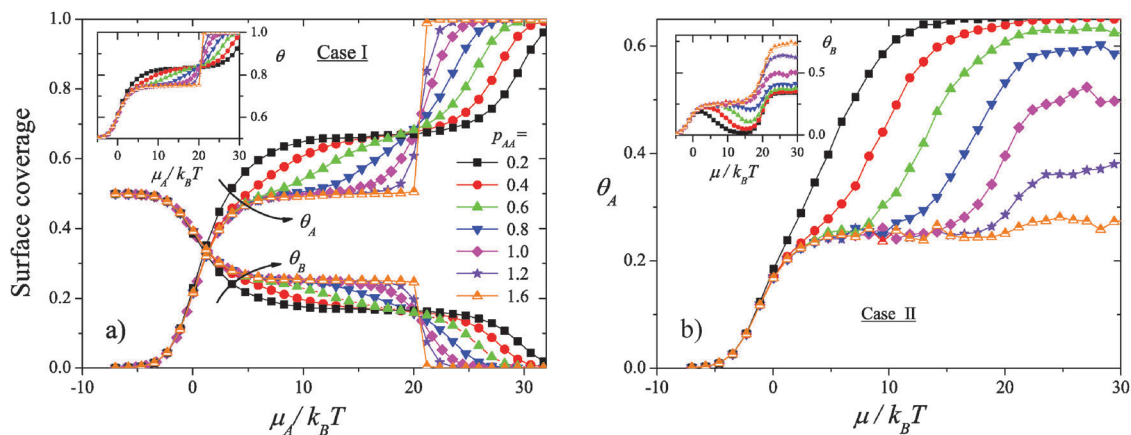
Fig. 9 One-dimensional mixture adsorption. (a) Partial and total (inset) adsorption isotherms for Case I. (b) Adsorption isotherms for the A and B (inset) species for Case II.

to zero energy, whereas B particles randomly occupy the rest of the sites. For values of $p_{AA} < 1$ the plateau becomes narrower, disappearing completely for $p_{AA} = 0.2$. A second plateau at $\theta = 2/3$, corresponding to a dimer-like structure, is observed for values of $p_{AA} < 0.6$. As in the two-dimensional case, a jump is observed in the adsorption isotherm for $p_{AA} > 1.0$. It is important to note that although a jump in the adsorption isotherm may be indicative of a condensation transition, it may not be the case in a one-dimensional confined fluid. It is well-known that no phase transition develops in a one-dimensional lattice when weak coupling between neighboring particles exists.[53] The full isotherm is shown in the inset of Fig. 9(a).

Fig. 9(b) corresponds to Case II, for $w_{AA} = w_{AB} = w_{BB} = 10.0\ k_BT$ and different values of p_{AA}. At these energies both the adsorption isotherms and the differential heat and the energy per site (not shown here for brevity) are in perfect agreement with the description of the two-dimensional case.

V. Conclusions

In this work, a lattice-gas model to study the adsorption of a mixture of particles with non-additive lateral interactions was presented. The traditional and widely used assumption of additivity in the lateral interaction energies between adatoms was replaced with a more realistic one, where the energy linking an atom with any of its nearest neighbors strongly depends on the state of occupancy in the first coordination sphere of that adatom, regardless of the species involved. The main objective was to analyze the effects of non-additive lateral interactions on the adsorption of a mixture and the competition between the adsorbed species. By using grand canonical MC simulation, the most relevant thermodynamic functions of adsorption (adsorption isotherms and differential heat of adsorption) were calculated. Three different cases were considered.

Case I: The competition of a species with non-additive interactions ($p_{AA} \neq 1$) and a non-interacting one ($w_{BB} = 0$) was analyzed. The chemical potential of the non-interacting species is held fixed throughout the adsorption process. For p_{AA}

less than one, structures are formed on the surface and the non-interacting species only occupies a half of the empty sites. However, for p_{AA} greater than one, the additive species is eventually expelled from the system due to the condensation of the other species. Thus, the non-additive species is imposed on the additive one.

Case II: The non-additive interaction is considered only between one of the species ($p_{AA} \neq 1$), with the rest of lateral interactions being additive ($p_{AB} = p_{BB} = 1$). Both species coexist at low coverage until a $c(2 \times 2)$ structure is formed by a mixture of both species. For $p_{AA} < 1.0$, as the chemical potential is increased, the additive species is initially expelled and a dimeric structure is formed by the non-additive one. For $p_{AA} > 1.0$ there is a partial expulsion of the non-additive particles from the $c(2 \times 2)$ structure coinciding with a strong increase of the additive species.

Case III: In this scheme, interspecies attractive and non-additive interactions are considered ($p_{AB} \neq 1$, $w_{AB} < 0$), keeping the rest of interactions additive ($p_{AA} = p_{BB} = 1$). The interspecies association is favored. The system presents condensation. As the coverage is increased, both species tend to be associated with them.

All the previous cases were also studied in one dimension. The features observed in the adsorption isotherms were similar to the cases reported here; however, they may not be associated with any phase transition as is expected of one-dimensional systems. In the case of honeycomb and triangular two-dimensional lattices, it is expected, when compared with a square geometry, the occurrence of different low temperature ordered phases in the adlayer. In fact, for square substrates and low temperatures, the adsorbate forms a $c(2 \times 2)$ phase at half coverage and this structure guides the formation of secondary phases for high values of the density (dimeric and tetrameric phases). In the case of honeycomb lattices, the adsorbate also exhibits a $c(2 \times 2)$ type of ordered structure at $\theta = 0.5$, and the behavior of the adsorption quantities is expected to be similar to the one corresponding to the square lattice. The situation is different for triangular lattices, where two structures are formed on the surface on the basis of the

well-known $(\sqrt{3} \times \sqrt{3})$ phase and its complementary $(\sqrt{3} \times \sqrt{3})^*$. Accordingly, a rich phase behaviour is expected of non-additive binary mixtures adsorbed on triangular lattices. Work in this line is in progress.

In summary, we found that the critical behavior of the system is strongly affected by the non-additivity. A more exact determination of the critical properties of the model (critical temperature and nature of the phase transition), based on an exhaustive analysis of finite-size scaling, will be the subject of future studies.

Acknowledgements

References

1 D. M. Ruthven, *Principles of Adsorption and Adsorption Processes*, Wiley, New York, 1984.
2 R. T. Yang, *Gas Separation by Adsorption Processes*, Butterworth, London, 1987.
3 L. K. Doraiswamy, *Prog. Surf. Sci.*, 1990, **37**, 1.
4 W. Rudzinski, W. A. Steele and G. Zgrablich, *Equilibria and Dynamics of Gas Adsorption on Heterogeneous Solid Surfaces*, Elsevier, Amsterdam, The Netherlands, 1997.
5 S. Sircar, *Langmuir*, 1991, **7**, 3065.
6 M. Heuchel, R. Q. Snurr and E. Buss, *Langmuir*, 1997, **13**, 6795.
7 K. Ayache, S. E. Jalili, L. J. Dunne, G. Manos and Z. Du, *Chem. Phys. Lett.*, 2002, **362**, 414.
8 L. J. Dunne, G. Manos and Z. Du, *Chem. Phys. Lett.*, 2003, **377**, 551.
9 M. Dávila, J. L. Riccardo and A. J. Ramirez-Pastor, *J. Chem. Phys.*, 2009, **130**, 174715.
10 M. Dávila, J. L. Riccardo and A. J. Ramirez-Pastor, *Chem. Phys. Lett.*, 2009, **477**, 402.
11 A. L. Myers, Molecular thermodynamics of adsorption of gas and liquid mixtures, in *Fundamental of Adsorption*, ed. A. J. Liapis, Engineering Foundation, New York, 1987.
12 B. Smit and T. L. M. Maesen, *Chem. Rev.*, 2008, **108**, 4125.
13 F. Gonzalez-Cavallero and M. L. Kerkeb, *Langmuir*, 1994, **10**, 1268.
14 J. A. Dunne, R. Mariwala, M. Rao, S. Sircar, R. J. Gorte and A. L. Myers, *Langmuir*, 1996, **12**, 5888.
15 J. A. Dunne, M. Rao, S. Sircar, R. J. Gorte and A. L. Myers, *Langmuir*, 1996, **12**, 5896.
16 W. A. Steele, *The Interaction of Gases with Solid Surfaces*, Pergamon Press, New York, 1974.
17 E. Alison Flood, *The Solid–Gas Interface*, M. Dekker Inc., New York, 1967.
18 V. P. Zhdanov, *Elementary Physicochemical Processes on Solid Surfaces*, Plenum Press, New York/London, 1991.
19 Y. K. Tovbin, *The Theory of Physical Chemistry processes at a Gas–Solid Interfaces*, Mir Publishers & CRC Press, Boca Raton, FL, 1991.
20 Y. K. Tovbin, *Langmuir*, 1997, **13**, 979.
21 Y. K. Tovbin, Application of Lattice-Gas Models to Describe Mixed-Gas Adsorption Equilibria on Heterogeneous Solid Surfaces, in *Equilibria and Dynamics of Gas Adsorption on Heterogeneous Solid Surfaces*, ed. W. Rudzinski, W. A. Steele and G. Zgrablich, Elsevier, Amsterdam, 1996.
22 E. V. Votyakov and Y. K. Tovbin, *Langmuir*, 1997, **13**, 1079.
23 K. Binder, *Monte Carlo methods in statistical physics: Topics in Current Physics*, Springer, Berlin, 1978, vol. 7.
24 K. Binder, *Rep. Prog. Phys.*, 1997, **60**, 448.
25 K. Binder and D. W. Heermann, *Monte Carlo Simulation in Statistical Physics. An Introduction*, Springer, Berlin, 1988.
26 P. Ungerer, B. Tavitian and A. Boutin, *Applications of Molecular Simulation in the Oil and Gas Industry: Monte Carlo Methods*, Editions Technip, Paris, 2005.
27 F. Bulnes, A. J. Ramirez-Pastor and V. D. Pereyra, *J. Mol. Catal. A: Chem.*, 2001, **167**, 129.
28 D. Nicholson and N. G. Parsonage, *Computer Simulation and the Statistical Mechanics of Adsorption*, Academic Press, London, 1982.
29 F. Bulnes, V. Pereyra and J. L. Riccardo, *Phys. Rev. E: Stat. Phys., Plasmas, Fluids, Relat. Interdiscip. Top.*, 1999, **58**, 86.
30 A. Patrykiejew, S. Sokolowski and K. Binder, *Surf. Sci. Rep.*, 2000, **37**, 207.
31 A. Milchev, *J. Chem. Phys.*, 1983, **78**, 1994.
32 A. Milchev and M. Paunov, *Surf. Sci.*, 1981, **108**, 25.
33 A. Milchev and K. Binder, *Surf. Sci.*, 1985, **164**, 1.
34 O. A. Pinto, A. J. Ramirez-Pastor and F. Nieto, *Surf. Sci.*, 2008, **602**, 1763.
35 O. A. Pinto, A. J. Ramirez-Pastor and F. Nieto, *Physica A*, 2010, **389**, 3456.
36 W. H. Ching, D. Huber, M. G. Lagally and G. C. Wang, *Surf. Sci.*, 1979, **77**, L497.
37 R. Imbihl, R. J. Behm, K. Chritmann, G. Ertl and T. Matsushima, *Surf. Sci.*, 1982, **117**, 257.
38 K. Binder and D. P. Landau, *Surf. Sci.*, 1981, **108**, 503.
39 L. C. A. Stoop, *Thin Solid Films*, 1983, **103**, 375.
40 K. Kaski, W. Kinzel and J. D. Gunton, *Phys. Rev. B: Condens. Matter Mater. Phys.*, 1983, **27**, 6777.
41 P. A. Rikvold, K. Kaski, J. D. Gunton and M. C. Yalabik, *Phys. Rev. B: Condens. Matter Mater. Phys.*, 1984, **29**, 6285.
42 F. H. Ree and C. F. Bender, *Phys. Rev. Lett.*, 1974, **32**, 85.
43 J. Kolaczkiewicz and E. Bauer, *Surf. Sci.*, 1985, **151**, 333.
44 R. Balog, B. Jørgensen, J. Wells, E. Lægsgaard, P. Hofmann, F. Besenbacher and L. Hornekær, *J. Am. Chem. Soc.*, 2009, **131**, 8744.
45 T. E. Felter and P. J. Estrup, *Phys. Rev. Lett.*, 1977, **38**, 1138.
46 F. Nieto and V. Pereyra, *Surf. Sci.*, 1997, **383**, 308.

47 F. Nieto and V. Pereyra, *Surf. Sci.*, 1998, **399**, 96.

48 O. A. Pinto, P. M. Pasinetti, A. J. Ramirez-Pastor and F. Nieto, *J. Chem. Phys.*, 2011, **134**, 064702.

49 O. A. Pinto, F. Nieto and A. J. Ramirez-Pastor, *Phys. Rev. E: Stat., Nonlinear, Soft Matter Phys.*, 2011, **84**, 061142.

50 G. D. Garcia, F. O. Sanchez-Varretti, F. Bulnes and A. J. Ramirez-Pastor, *Surf. Sci.*, 2012, **606**, 83.

51 N. Metropolis, A. W. Rosenbluth, M. N. Rosenbluth, A. H. Teller and E. Teller, *J. Chem. Phys.*, 1953, **21**, 1087.

52 P. Rinaldi, F. Bulnes, A. J. Ramirez-Pastor and G. Zgrablich, *Surf. Sci.*, 2008, **602**, 1783.

53 T. L. Hill, *An Introduction to Statistical Thermodynamics*, Addison-Wesley Publishing Company, Reading, MA, 1960.

54 V. A. Bakaev and W. A. Steele, *Langmuir*, 1992, **8**, 148.

55 A. J. Ramirez-Pastor and F. Bulnes, *Physica A*, 2000, **283**, 198.

56 P. M. Pasinetti, J. L. Riccardo and A. J. Ramirez-Pastor, *Physica A*, 2005, **355**, 383.

57 R. A. Trasca, M. M. Calbi and M. W. Cole, *Phys. Rev. E: Stat., Nonlinear, Soft Matter Phys.*, 2002, **65**, 061607.

58 R. A. Trasca, M. M. Calbi, M. W. Cole and J. L. Riccardo, *Phys. Rev. E: Stat., Nonlinear, Soft Matter Phys.*, 2004, **69**, 011605.